Received: 16 June 2022 | Accepted: 8 December 2022 | Published online: 19 February 2023

DOI: 10.1002/csc2.20899

Crop Science

ORIGINAL ARTICLE

Crop Physiology & Metabolism

Assessing axial and temporal effects of the leaf sheath on the flexural stiffness of large-grain stems

Jared Hale[1] | **Spencer Webb**[1] | **Nathan Hale**[1] | **Christopher Stubbs**[2] | **Douglas Cook**[1]

[1]Department of Mechanical Engineering, Brigham Young University, Provo, UT, USA

[2]School of Computer Sciences and Engineering, Fairleigh Dickinson University, Teaneck, NJ, USA

Correspondence
Department of Mechanical Engineering, Brigham Young University, 350 Engineering Building, Provo, UT 84602, USA.
Email: ddc971@byu.edu

Assigned to Associate Editor Carlos Messina.

Funding information
National Institute of Food and Agriculture, Grant/Award Number: 2022-67022-37870; National Science Foundation, Grant/Award Number: 2046669; Brigham Young University College of Engineering

Abstract

The leaf sheath of many plants has been observed to influence both stiffness and ultimate strength. For example, the sheath has been observed to be closely related to "greensnap" (or "brittle-snap") failure of *Zea mays*. The goal of this study was to develop a method for assessing longitudinal and temporal patterns of sheath influence on flexural stiffness. This metric was chosen because it has been shown to be predictive of ultimate bending strength. A three-point bending test method was developed for assessing the longitudinal and temporal influence of the sheath on flexural stiffness of *Zea mays*. Comparisons between pairs of tests at the same location (sheath present vs. absent) were performed. Four types of maize were tested. The sheath had a statistically significant influence on bending. Sheath influence appears to be closely related to maturity since both spatial and temporal patterns of influence mirror the sigmoidal maturation patterns previously observed in maize stalks. The paired nature of this method increases statistical significance and allows for multiple tests along the length of the stalk. Results indicate that the influence of the sheath changes over the life span of the *Zea mays* in parallel with maturation patterns. However, further studies will be needed to confirm this hypothesis more broadly and to study additional issues such as heritability and the influence of genotype and environment on sheath effects. Due to the common architecture of *Poacea* plants, this method can be used to provide new insights on sheath influences of various species.

1 | INTRODUCTION

The clasping leaf sheath has been recognized as playing a role in the mechanical response of *Poacea* species such as *Avena sativa* (oats), *Arundinaria tecta* (switchcane), as well as plants in other families, such as palms (Isnard & Rowe, 2008; Niklas, 1990, 1998). Recent studies have examined the influence of the leaf sheath on the stiffness and strength on wheat and oat stems (Wu & Ma, 2019). The leaf sheath has also been observed to play a role in a phenomenon known as maize greensnap (wind-induced fracture of the stalk during rapid growth) (Elmore & Ferguson, 1999; Elmore et al., 2003). Finally, it has been observed that the presence of sheath blight increases the lodging rate in rice (Wu et al., 2012).

The growth patterns of *Poacea* plants follow a bottom-up progression in which lower internodes elongate first, while upper internodes elongate last (Sharman, 1942). Studies of maize growth dynamics have revealed that both leaf development (including the sheath) and internode elongation follow sigmoidal or "S" shaped curves (Fournier & Andrieu, 2000; Morrison et al., 1994).

While the growth patterns of grain plants are well-documented, our overall understanding of leaf/sheath interactions remains relatively sparse. For example, Hill (2011) attempted to predict greensnap failure, but concluded that it was not yet possible to predict greensnap susceptibility. A recent study reported that maize stalks are not optimally tapered to resist bending loads (Stubbs, Seegmiller et al., 2020). However, that study examined stalks in the absence of sheaths.

A deeper understanding of sheath/stalk interactions is needed, but existing bending test methods and prior studies are inadequate. For example, Niklas studied the influence on two cultivars of *Avena satvia*, noting that the influence of the leaf sheath changed with tissue maturity, and along the length of the stalk (Niklas, 1990). That study made use of a fairly complex experimental apparatus and lacked a statistical analysis. The values reported in that study were also based on equations that modeled the stem as a solid cylinder. However, because the inner pith tissues are much more compliant than rind tissues (Stubbs et al., 2019; Stubbs, Larson, & Cook, 2020) the solid cylinder assumption induces significant errors in the calculated values for modulus of elasticity and flexural stiffness.

Previous studies that attempted to quantify sheath influence were either destructive (Isnard & Rowe, 2008; Wu & Ma, 2019), used hanging weights (Isnard & Rowe, 2008; Niklas, 1998), or used relatively complex vibratory methods (Niklas, 1990). Most importantly, these prior studies generally provided information only at the level of the entire stalk. Thus, those studies are not suited to assess how the sheath influence varies along the stalk. This is an important limitation, since the literature on stalk/sheath maturation suggests that the influence of the sheath may vary according to the tissue maturation of the stalk. Whole stalk measurements thus may obscure longitudinal patterns that are important for understanding the spatial and temporal influence of the sheath on stalk strength and flexibility.

The development of a robust testing methodology will enable future studies aimed at examining the influence of the leaf sheath in greater detail. For example, it has been proposed that further insights into the mechanisms of greensnap could enable metrics for predicting the susceptibility of maize to greensnap failure (Hill, 2011). Such metrics could accelerate genetic gain in lodging resistance, hence improving yield.

The first purpose of this study was to develop a technique for more quickly measuring the influence of the sheath as a function of axial position along the stalk of large grains such as maize and sorghum. The second purpose was to deploy this method to understand more about the role of the leaf sheath on maize stalk stiffness. The characteristic of flexural stiffness (also known as flexural rigidity) was chosen for two reasons. First, individual flexural stiffness tests are non-destructive. This allows for paired testing between the cases of sheath present vs. absent, which increases statistical power. Second, flexural stiffness has been found to be an excellent predictor of stalk strength in maize (Robertson et al., 2016).

Core Ideas

- Leaf sheaths provide structural support to maize stalks.
- Leaf sheaths influence varies spatially and temporally.
- A new three-point bending test provides high spatial resolution as well as high statistical power.
- Leaf sheath influences mirror maturation patterns of the stalk.

2 | MATERIALS AND METHODS

2.1 | Maize plants

Four types of commercial maize were used in this study, including two varieties of field corn (Vigor Root and Silver Queen), one type of sweet corn (Extra Early), and one type of flint corn (Fiesta Ornamental). For brevity, these varieties are denoted as VR, SQ, EE, and FO, respectively. Plants were grown in Spanish Fork, Utah in a single location and at a single planting density as these variables were not of interest in this study. Plants were grown using the plastic mulch method (Tarara, 2000). Plants were irrigated as needed, typically 2–3 times per week.

2.2 | Specimen preparation

Stalks were harvested from the field immediately before testing. On each day of testing, a sample of seven stalks was chosen from each variety. Stalks were selected from random locations within the field, but not from row ends. Pruning shears were used to cut the stalk just below the brace roots. Following collection, all stalks were taken directly to the laboratory for testing.

To prepare for testing, the leaf blades were removed just above the collar using scissors. For testing alignment purposes, stalks were marked with a thin black line every 10 cm starting at the basal node using an indelible felt marker.

2.3 | Flexural bending tests

Three-point bending tests were performed using a universal testing machine (Model 3340 Series, Instron). Traditionally, three-point bending tests are performed with a load point

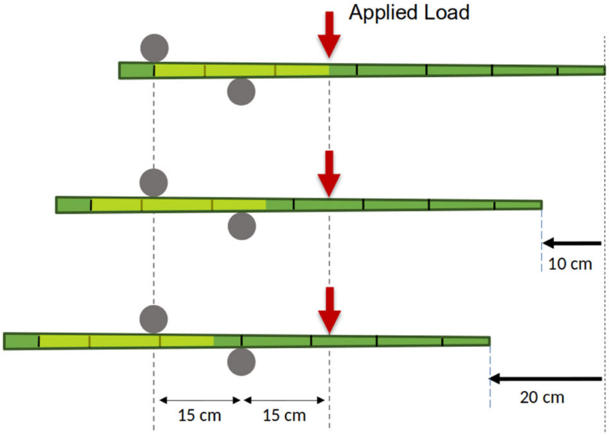

FIGURE 1 An illustration of the test arrangement used in this study. Supports are represented by gray circles while the red arrow represents the applied force. Supports are fixed throughout the experiment while the stalk is shifted left by 10 cm at each stage. The first tested region is highlighted to illustrate the overlapping nature of tests.

centered between the two supports. However, this approach was not appropriate in this case because the apical portions of the stalk were sometimes too weak to support the stalk's ownweight. Instead, both supports were placed on one side of the load point, as shown in Figure 1. This configuration is structurally equivalent to a traditional three-point bending test. This approach allowed the stronger basal region to support the weight of the weaker apical section.

Distances between supports/loads were the same for all tests. Supports were placed 15 and 30 cm to the left of the loading anvil. The loading anvil was slowly lowered until the loading anvil made contact with the stalk and induced a slight bending displacement. At this point, the force and displacement were set to zero. The machine then executed three displacement cycles. Each cycle applied a 2 mm displacement to the stalk and then returned to the zero position. This small value for displacement was chosen because it allowed flexural data to be collected without causing any observable damage to the stalk or sheath (i.e., the force/deformation path was highly linear). After testing a particular section, the stalk was moved 10 cm to the left, as shown in Figure 1. This process was repeated along the length of each stalk.

Stalks were first tested with the leaf sheaths intact. After the entire stalk had been tested, all the leaf sheaths were removed by scoring the outside of the sheath at the node and carefully peeling away the sheath. During the sheath removal process, marks were transferred to the stalk. Each stalk was then tested again at each of the same locations as the initial tests. In this way, each 30 cm section of the stalk was tested with sheaths present and absent and the testing process was repeated at 10 cm intervals along the entire stalk.

2.4 | Flexural stiffness calculations

Flexural stiffness (or flexural rigidity) is typically defined in engineering textbooks as *EI*: the product of the Young's Modulus (*E*) and the area moment of inertia (*I*). Flexural stiffness is most easily obtained by combining force/deformation measurements with the equation for deflection of a beam in three-point bending. Under this approach, the following equation is used to calculate the flexural stiffness:

$$\delta = \frac{PL^3}{48EI} \tag{1}$$

Here P represents the applied force, L is the span between supports, and δ is the deflection at the point of the applied load. This approach relies upon two important assumptions: first, that E is constant within each cross-section of the beam, and second, that both the geometry and the material properties are constant along the length of the beam. Neither of these assumptions is typically true for plant stems. A previous study showed that tissue stiffness variation can be accounted for using a different form for the moment of inertia (Stubbs et al., 2018). In that formulation, the material stiffness (E) is allowed to vary as functions of x and y within the cross-section. Integrating the material stiffness over the cross-sectional area (dA) produces the material-weighted moment of inertia (I_E):

$$I_E = \int E\,(x, y)\, y^2 dA \tag{2}$$

The material-weighted moment of inertia represents the cross-sectional resistance to bending. In other words, *IE* captures the flexural stiffness when material properties vary across the cross-section. If *IE* is allowed to vary along the length of the stalk, we can write an expression for the deflection using Castigliano's Theorem:

$$\delta = \int \frac{\partial}{\partial P}\left(\frac{M(z)}{I_E(z)}\right) dz \tag{3}$$

Unfortunately, this equation cannot be evaluated since we do not know the axial variation of *IE*. However, if we use a relatively short test span and assume that *IE* is constant within the test span, we obtain an equation that is very similar to the standard form:

$$\delta = \frac{PL^3}{48I_E} \tag{4}$$

This can be solved for the flexural stiffness as:

$$I_E = \frac{PL^3}{48\delta} \tag{5}$$

This approach produces an aggregate flexural stiffness (I_E) for each test region shown in Figure 1. The key to this approach is the use of *overlapping* sections of 30 cm each. This approach allows the assessment of flexural stiffness along the length of the stalk.

2.5 | Data analysis

The data produced by the experiments described above consisted of two sets of flexural stiffness measurements along the length of each stalk: one set representing the flexural stiffness with the sheath present, and a corresponding set of measurements at the same locations, but with the sheath removed. Additional data dimensions included the type of maize and the test date of each data set.

A simple paired *t*-test was used to assess the overall difference in flexural stiffness between the sheathed and unsheathed conditions. This approach neglects factors such as variety, date, or axial position, but it provides an overall assessment of the influence of the sheath. Paired *t*-tests were performed by first calculating the percentage difference between sheathed and unsheathed tests according to Equation (6) below. The null hypothesis was that the sheath had no influence on stiffness:

$$\text{Parcent sheath influence} = \frac{EI_{\text{with sheath}} - EI_{\text{no sheath}}}{EI_{\text{with sheath}}} 100 \quad (6)$$

A simple analysis of variance was performed to rank the three major variables in terms of their effect on sheath influence. These variables included axial position along the stalk (x), time (t) of testing in terms of days since planting, and variety.

The effect of the sheath along the length of the stalk and over time was analyzed using a nonlinear regression approach. The growth and development of maize internodes and sheaths often follow a sigmoidal ('S' shaped) curve (Fournier & Andrieu, 2000). Thus, a sigmoidal curve was used as the basis for describing the influence of the leaf sheath on stem stiffness as a function of axial position.

The sigmoidal curve has four key variables, which are illustrated in Equation (7) and in Figure 2. Variable "a" is the upper asymptote, which represents the maximum sheath influence. Variable b is the lower asymptote, which represents the minimum sheath effect. Both a and b have units of percent. Variable c is related to the rate of transition from low to high effect. Lastly, d indicates the point of inflection, the point of the maximum rate of change, and the point along the stalk where the sheath has an influence of 50%. Units of millimeters were used for variables c and d.

$$f(x) = \frac{a-b}{1+e^{(d-x)/c}} + b \quad (7)$$

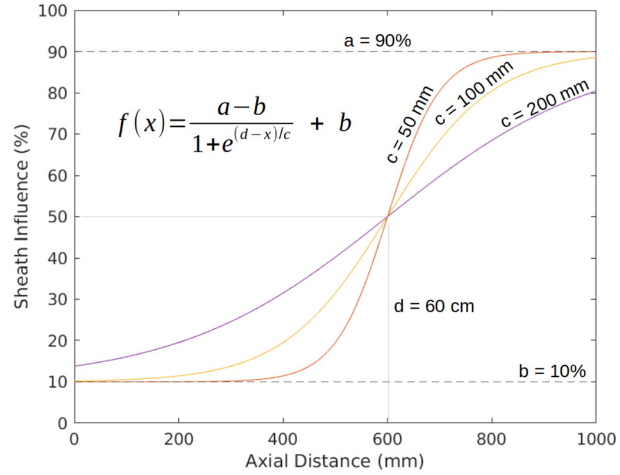

FIGURE 2 Three sigmoid curves with their associated coefficient values and the sigmoid curve equation.

Equation (7) captures the spatial influence of the sheath on stalk stiffness for a given variety at a specific moment in time. This formulation was used to perform an exploratory analysis of the patterns exhibited across time and between varieties.

Equation (7) was generalized to account for temporal effects (t) and the influence of variety (V_i). To do this, each coefficient (a, b, c, d) in Equation (7) was expanded as a linear function of time and variety. This model is summarized in Equations (8) and (9a–d):

$$f(x) = \frac{A-B}{1+e^{\frac{(D-x)}{C}}} + B \quad (8)$$

$$A = a_{0G} + a_{1G}t + \sum_{i=1}^{4} V_i\left(a_0^i + a_1^i t\right) \quad (9a)$$

$$B = b_{0G} + b_{1G}t + \sum_{i=1}^{4} V_i\left(b_0^i + b_1^i t\right) \quad (9b)$$

$$C = c_{0G} + c_{1G}t + \sum_{i=1}^{4} V_i\left(c_0^i + c_1^i t\right) \quad (9c)$$

$$D = d_{0G} + d_{1G}t + \sum_{i=1}^{4} V_i\left(d_0^i + d_1^i t\right) \quad (9d)$$

Here the subscript G stands for "generic" as it captures trends that are independent of variety. The index i refers to variety and the influence of variety was captured using a categorical variable V_i (0 or 1) along with variety-specific intercept ("0" subscripts) and slope terms

("1" subscripts). Superscripts were used to link coefficients with their respective variety.

A constrained optimization program was used to calculate the best-fit values for each of the model coefficients. Equation (7) required just four coefficients, but the use of Equations (8) and (9) required optimizing for 40 coefficients. The optimization routine minimized the SSE statistic (sum of squared errors between the model and the data). Optimization was performed using the constrained nonlinear optimization function "mfmincon()" in the commercial software package MATLAB (MathWorks). Constraints were used to keep each parameter within physically realistic bounds (all a and b coefficients were held between 0 and 100, c and d coefficients were restricted between 0 and the stalk height).

Statistical models operated on three levels. At the first level, Equation (7) was applied to data collected for a single variety at a specific time point. These "snapshot" models capture nonlinear spatial variation in sheath influence but do not account for time or variety. At the second level, spatial patterns and time were considered, but variety was ignored. This approach utilized Equation (8), but involved only the "G" subscript terms in Equation (9). Finally, spatial, temporal, and variety effects were considered by using Equations (8) and (9) with all terms included.

3 | RESULTS

3.1 | Overall influence of sheath by variety

As described in the methods section, the influence of the sheath was quantified as the percent difference in relation to the flexural stiffness measured with the sheath present. For each variety tested, the leaf sheath exhibited a statistically significant effect on the stiffness of the stem. Figure 3 shows the distributions of the relative effect of the leaf sheath for the varieties tested in this study, regardless of other factors. Paired t-tests indicated that the influence of the sheath was highly significant in all varieties ($p < 0.001$ for all tests). However, the influence of the sheath varies between 0% and at least 75% for each variety. Much of this variation is due to the remaining experimental factors as well as experimental uncertainty. Analysis of variance revealed that each of the variables significantly affected sheath influence, with spatial location (x) having the strongest effect on sheath influence, followed by time (t), and lastly by variety. Table 1 provides the ANOVA table of results.

3.2 | Level 1 modeling: Spatial variation in sheath influence

The spatial influence of the sheath on overall stem stiffness was clearly evident when the variety and date were held constant. For each date/variety pair, the influence of the sheath increased with distance from the base of the stalk. A typical example of this characteristic spatial pattern is shown in Figure 4, in which the distance from the base of the stalk increases from left to right, and the vertical axis indicates the influence of the sheath.

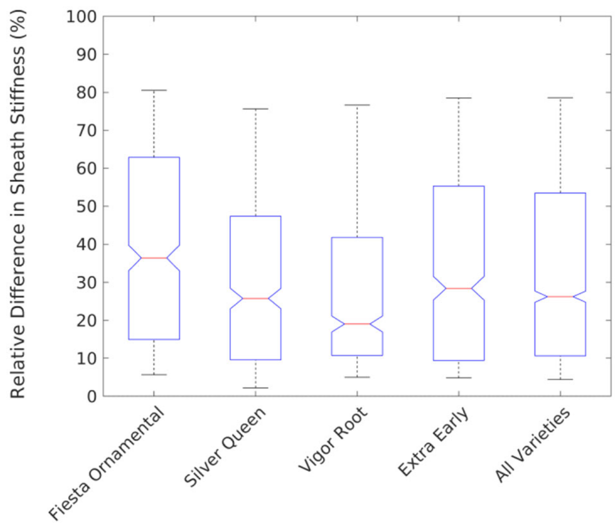

FIGURE 3 Box plots depicting the influence of the leaf sheath on flexural stiffness for each variety tested, and all varieties combined (last box). Notches indicate statistical significance.

TABLE 1 ANOVA Table for a simple linear model containing the three variables of interest.

	Sums squared	*Df*	MSE	*p* value
Variety	2.64	3	0.88	0.0000
Time	37.61	1	37.61	0.0000
Test Location	53.40	1	53.40	0.0000
Error	75.74	2018		

Note: The R^2 value for the linear model containing these three variables was 0.52.

A total of 29 "snapshot" sigmoidal fits of this type were performed using Equation 7 (one for each date/variety pair). The $R2$ values were statistically significant for every snapshot model, which indicates that leaf sheath influence follows the same sigmoidal pattern that has been used to describe node elongation (9,10). Across all models, the median $R2$ value was 0.69, with a mean and standard deviation of 0.65 and 0.15, respectively. All 29 charts with the associated $R2$ values are available in the supplementary data that accompanies this paper.

The 29 snapshot models required 116 unique coefficients ($29 \times 4 = 116$). This collection of models accounted for 74% of the variance in the data. This approach captured variety-specific and temporal effects implicitly rather than explicitly.

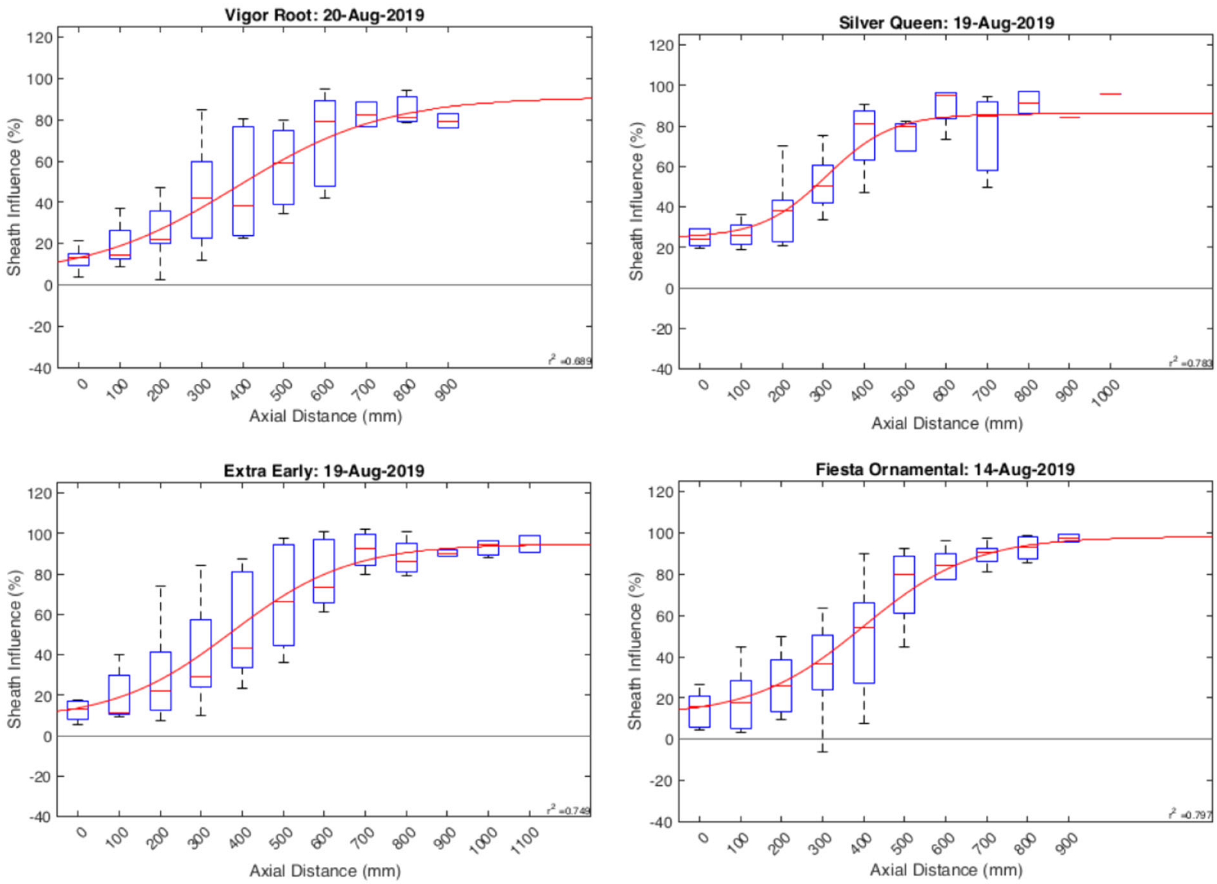

FIGURE 4 Representative charts for each variety showing the sigmoid curve fitted to test results as a function of axial position. Additional charts available in the supplementary data that accompanies this paper.

3.3 | Using Level 1 models to understand temporal patterns

While Level 1 (snapshot) models did not model temporal effects explicitly, distinct temporal patterns were apparent in both boxplots and changes in snapshot model shape over time. Figure 5 shows two snapshop curves at two-time points and for two different varieties. As seen in Figure 5, at 55 days after planting the influence of the sheath varies spatially with a minimum influence of approximately 10% in each variety and a maximum influence of approximately 90%. In contrast, the sigmoid curves at 110 days after planting indicate a maximum sheath influence of only about 40%–50%.

Sigmoid curve shifts over time can be understood more clearly by plotting the values of snapshot model coefficients (Equation 7) as functions of time. Recall from the methods section that parameters *a* and *b* indicated the minimum and maximum influence of the sheath, while parameters *c* and *d* indicate the rate of increase and location of the inflection point (see Figure 2 for graphical representations of each coefficient). Figure 6 provides plots of each coefficient as a function of time and variety. As seen in black in the top row of Figure 6, the coefficient *a* (the maximum level of sheath influence) exhibited a statistically significant decrease over time for each variety. In contrast, coefficient *b* (gray, minimum level of sheath influence) was found to be relatively stable over time.

Coefficient *d* captures the point of inflection of the sigmoid curve. This coefficient (shown in black in the bottom row of Figure 6), exhibited a statistically significant increase over time for each variety. The temporal patterns of coefficient *c* were relatively weak. This data indicates that the overall influence of the leaf sheath (the difference between *a* and *b*) decreases as time progresses while the point of inflection moves upward along the stalk as time increases. Coefficients (*b* and *c*) did not have a significant pattern across time.

3.4 | Level 2 modeling: Generic model with temporal effects

The generic model simultaneously captured all of the time dependencies shown in Figure 6. The generic model is provided in Equations (8) and (9) where only the “G” subscript terms in Equation (9) are used. The generic model consisted of 8 coefficients and produced an R^2 value of 0.59. Unlike

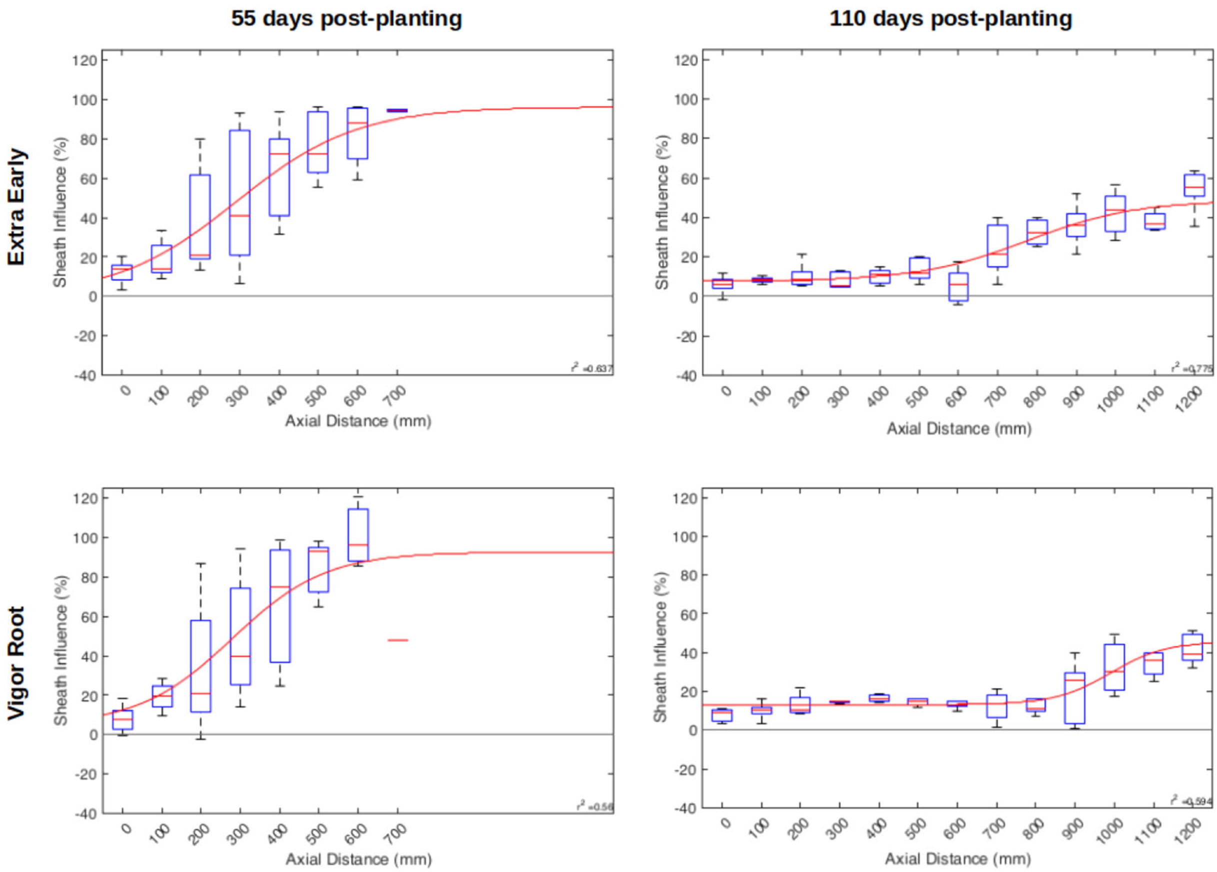

FIGURE 5 Data and sigmoid curves for two varieties at 55 days and 110 days post-planting.

linear models, where terms can be omitted, the structure of the sigmoid function requires that all coefficients be included. Nevertheless, not all coefficients were statistically significant. The variance/covariance matrix was used to obtain 95% confidence intervals on each coefficient (Bonferonni correction was included to account for the number of tests). This analysis revealed that all a, b, and d coefficients were statistically nonzero while both of the b coefficients were not significantly different from 0 (Figure 8).

The statistically significant temporal patterns predicted by the generic model are illustrated graphically in Figure 7. The arrow indicates the passage of time, with sigmoidal curves of sheath influence depicted at four equally spaced time points. The point of inflection (d) moves upward along the stalk as the upper asymptote (a) simultaneously moves downward and the slope at the point of inflection (c) decreases with time. These results are independent of variety.

3.5 | Level 3 modeling: Temporal and variety effects included

Including both generic and variety-specific terms (an additional 32 terms over the generic model) increased the R^2 value modestly from 0.59 (generic model) to 0.67. The individual sum squared total and error terms for both generic and variety-specific models are provided in Table 2. This table also provides SST and SSE values broken down by variety which reveals that some variety-specific models differed from the generic model more than others. For example, the generic model predicted 67% of the variance in the Extra Early variety. Adding 8 additional hybrid-specific terms to the model increased the predictive capability to just 70%. In contrast, the generic model captured just 51% of the variety Silver Queen, and adding variety-specific terms increased the predictive capability to 68% (an increase of 17%).

Although this study was not designed to identify differences between varieties, the variance/covariance matrix of the models used in this study was used to obtain confidence intervals for individual coefficients to illustrate that variety-specific differences were detected. Confidence intervals for generic model and variety-specific models are shown in Figure 8. For convenience in making comparisons, the variety-specific coefficients in Figure 8 are shown as net coefficients: generic plus variety-specific terms rather than as separate generic and variety-specific coefficients as used in Equation (9). Figure 8 shows that the vast majority of a, c, and d coefficients were statistically significant, while

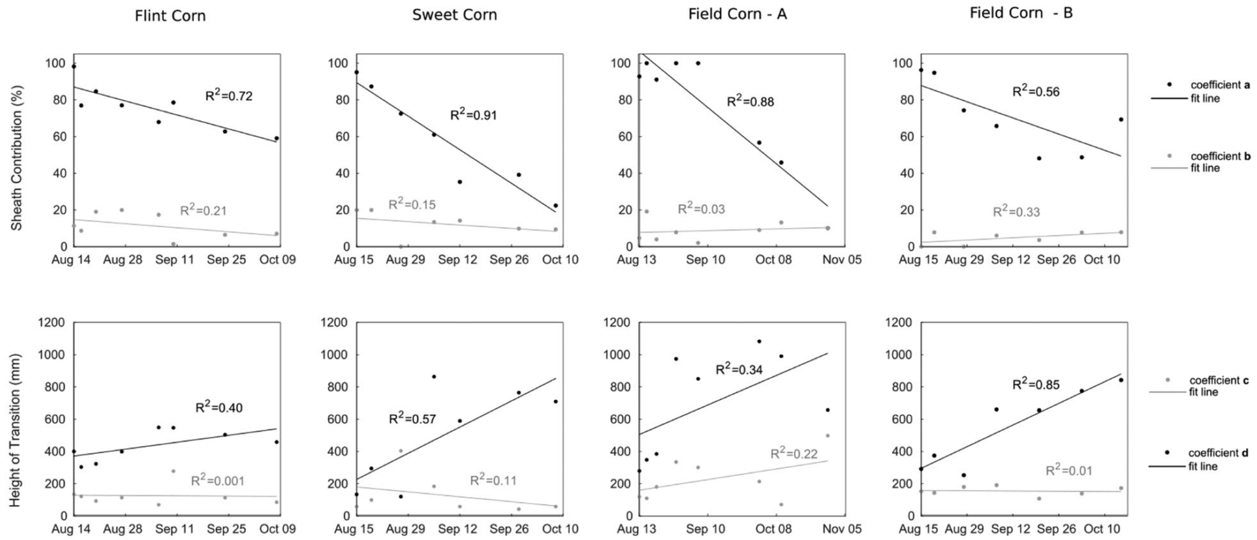

FIGURE 6 Plots of coefficient values over time for each of the four varieties. Consistent patterns were observed for coefficients *a* and *d* (shown in black). In contrast, inconsistent patterns were observed for coefficients *b* and *c* (shown in gray).

TABLE 2 Sums of squared terms by variety for both generic and variety-specific models.

		SSE		R^2		
Variety	**SST**	**Generic model**	**Variety-specific**	**Generic model**	**Hybrid-specific**	**Sample size**
Extra early	41.5	13.6	12.6	0.67	0.70	524
Vigor root	39.9	15.8	14.9	0.60	0.63	535
Fiesta O.	42.3	17.8	13.5	0.58	0.68	497
Silver Q.	35.0	17.1	11.3	0.51	0.68	468
Total	158.6	64.4	52.3	0.59	0.67	2024

Abbreviations: SST, sum of squares total; SSE, sum of squares error.

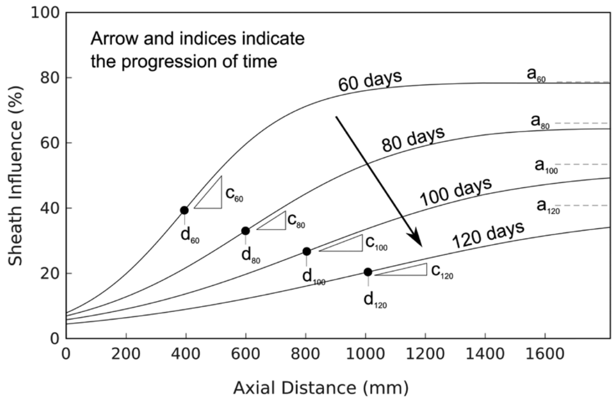

FIGURE 7 The progression of sigmoid curves as a function of time within the generic model. The statistically significant coefficients are shown at times of 60, 80, 100, and 120 days.

the *b* coefficients typically were not. Several variety-specific differences were detected, though these should be interpreted as illustrative only due to the limited scope of this experiment.

4 | DISCUSSION

Previous studies have demonstrated that the growth and development of maize follow sigmoidal patterns in both space and time (Fournier & Andrieu, 2000; Morrison et al., 1994; Stubbs et al., 2018). When comparing maturity across internodes, tissue maturity is highest at the base, and lowest at the apex. The data in this study suggest that the influence of the sheath is correlated with maturity, since both the influence of the sheath and patterns of maturity exhibit similar temporal patterns.

The generic model captured strong temporal patterns. With just eight parameters, this model captured 59% of the variation in sheath influence. Including variety-specific effects required an additional 32 coefficients, but only predicted an additional 8% in variance. Finally, the use of 29 snapshot models required an additional 120 coefficients, but only predicted 7% of the additional variance. While more research is needed, the major factors that determine the influence of the leaf sheath appear to be axial location and maturation (i.e., the passage of time). Variety appears to have a relatively minor effect, but data from this study suggests that variety effects

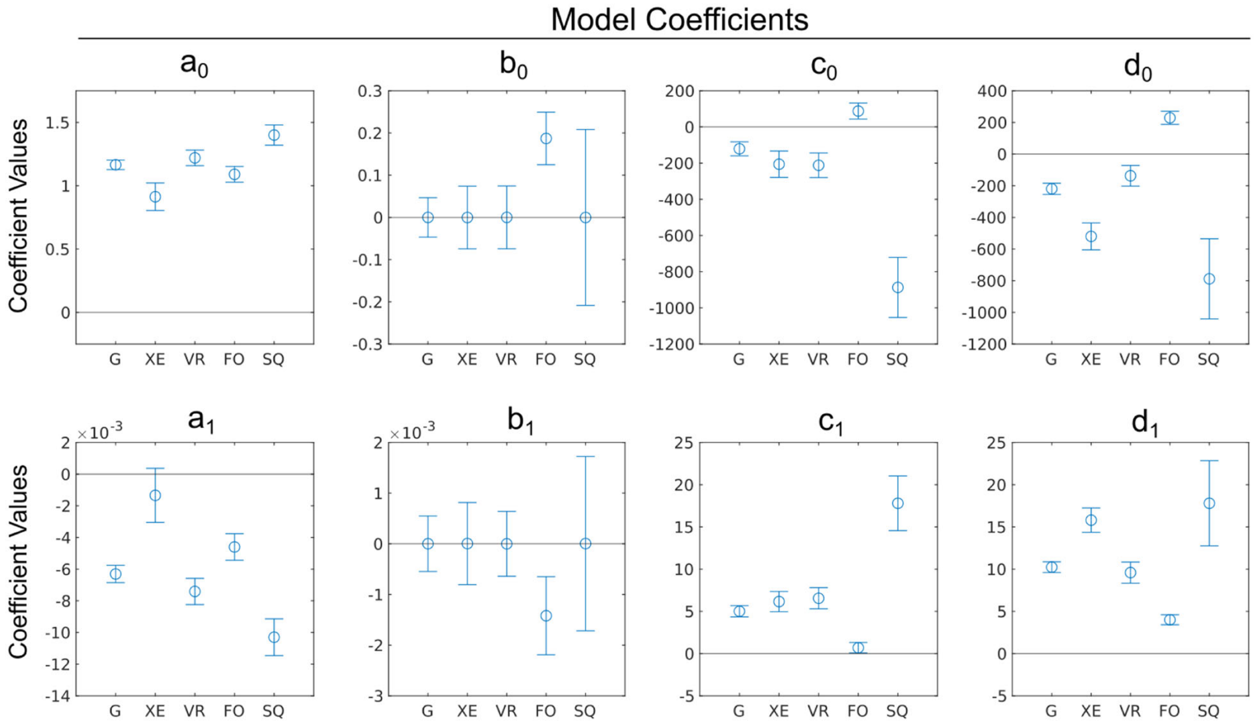

FIGURE 8 95% confidence intervals with Bonferroni corrections for the offset and slope coefficients for generic (G) and variety-specific model coefficients.

can also be statistically significant. Agronomic factors such as planting density, nutrient content, and field management were not investigated in this study but should be explored in future studies.

Dissection and qualitative examination of maize internodes revealed that immature tissues are soft, flexible, and have relatively low strength. In contrast, mature tissues are hard, inflexible, and appear to have higher strength. These observations, when combined with the data collected in this study suggest that the leaf sheath provides critical structural support for these immature tissues. Thus, as the tissues mature, the influence of the sheath decreases. This is likely related to mechanical changes in the sheath due to the remobilization of carbon from the leaf sheath as senescence progresses. While more focused research is needed to gain further insight, these observations likely have implications for future studies on the growth and development of grain species, and for studies focused on greensnap maize failure (Hill, 2011).

4.1 | Practical considerations

As with all test methods, this method has advantages and disadvantages. Advantages of this test method include the following: (1) minimal sample preparation; (2) the test does not induce structural damage of the specimen (though it requires removal of the leaf sheath); (3) the test supports are fixed throughout the test, which results in significant time savings over methods which require adjustment of the supports for each test (Robertson et al., 2014, 2015) (4) spatial resolution can be refined as desired by shortening the shift distance between tests (see Figure 1). For example, a shift distance of 5 cm would double the spatial resolution presented in this study; (5) the paired nature of the test increases statistical significance.

Disadvantages of this test method include the following; (1) the removal of the sheath can be somewhat time-consuming; (2) the attainment of high spatial resolution along the stalk increases the number of tests that must be performed and may cause a degradation in data quality as a shorter span increases the tendency for transverse compression of the stalk (Robertson et al., 2014, 2015; Stubbs et al., 2018); (3) the test requires a non-standard three-point bending test configuration. A complete test series of a single stalk required approximately 15 min to complete.

4.2 | Limitations and future research

The purpose of this study was methodological development, not to specifically quantify the influence of sheath on any particular variety or at any particular period of growth. Hence, some factors that may influence sheath/stalk interactions were not quantified nor varied. For example, field replicates and multiple growing environments were not used in this study and time was quantified using regular dates rather than by using growth-degree-units or phyllochrons. Planting density was held constant and only four varieties were investigated. The measurement uncertainty of the testing method was not quantified (Nelson et al., 2019). In spite of these limitations, this preliminary study demonstrates that the leaf sheath exerts a strong effect on the flexibility of maize stalks and suggests that the leaf sheath may also have a strong influence on the mechanical resilience of the stalk/sheath structure. This study also provides a clear methodology and framework for future studies that may examine differences between varieties, the influence of environment and field management, and the influence of time and temperature on the sheath effect.

Dissection of maize internode and observed differences between immature and mature tissues, including tissue stiffness, flexibility, and strength were only qualitative in nature (and hence were not included in the results section). However, these observations provide valuable insights for future researchers. In addition, this study did not seek to quantify the mechanical differences between immature and mature tissues. Such measurements will allow for a more complete description of the phenomena observed, and allow a more comprehensive description of the tissue maturation process. Significant methodological development will need to be performed in order to enable such measurements. Thus, future research in this area will need to focus first on the development of testing methodologies, as well as the application of these methodologies to the study of maize tissue development.

Finally, field-based measurement of stem stiffness may provide an alternative means of assessing the influence of the leaf sheath on flexural stiffness. A number of devices have been developed for flexing plants (Erndwein et al., 2020). The use of such devices would eliminate the need for laboratory measurements and would make use of the plants' natural root/soil boundary conditions. On the other hand, the soil itself can be an apparent source of flexure (Reneau et al., 2020), so this approach can introduce additional sources of error to the measurement process (Nelson et al., 2019). Additional research will be needed to develop a field-based protocol for such measurements. For example, the DARLING device has been used to perform in-field flexural measurements (Cook et al., 2019; Reneau et al., 2020). This study provides valuable guidance for such follow-on studies.

5 | CONCLUSIONS

This paper provides a description of a testing methodology that can be used to quantify the influence of the leaf sheath along two important dimensions: along the length of the stem, and across time. Results from preliminary tests indicate that the leaf sheath of maize plays an important structural role by increasing stem stiffness (and likely also increasing stalk strength). The influence of the sheath was observed to decrease over time, both locally at the individual internodes, and globally, across the entire length of the stem. The data collected in this study indicated that the leaf sheath significantly increased stem stiffness in each variety tested. Future studies are needed to fully understand the effects of the leaf sheath on issues such as greensnap failure and tissue maturation.

AUTHOR CONTRIBUTIONS

Jared Hale: Data curation; formal analysis; investigation; software; visualization; writing – original draft. **Spencer Webb**: Data curation; investigation; project administration; validation. **Nathan Hale**: Data curation; investigation; methodology; project administration; validation. **Christopher J Stubbs**: Conceptualization; investigation; methodology; supervision; validation. **Douglas Cook**: Conceptualization; funding acquisition; investigation; methodology; project administration; resources; supervision; validation; writing – original draft; writing – review & editing.

ACKNOWLEDGMENTS

This research was supported in part by funding from the National Science Foundation (award 2046669), the US Department of Agriculture (award 2022-67022-37870), and internal funding for undergraduate research from the Ira A. Fulton College of Engineering at Brigham Young University.

CONFLICT OF INTEREST STATEMENT

The authors declare no conflicts of interest.

DATA AVAILABILITY STATEMENT

The datasets during and/or analyzed during the current study are available from the corresponding author upon reasonable request.

ORCID

Douglas Cook https://orcid.org/0000-0002-1731-1978

REFERENCES

Cook, D. D., de la Chapelle, W., Lin, T. C., Lee, S. Y., Sun, W., & Robertson, D. J. (2019). DARLING: A device for assessing resistance to lodging in grain crops. *Plant Methods*, *15*(1), 1–8. https://doi.org/10.1186/s13007-019-0488-7

Elmore, R. W., & Ferguson, R. B. (1999). Mid-season stalk breakage in corn: Hybrid and environmental factors. *Journal of Production Agriculture*, *12*(2), 293–299. https://doi.org/10.2134/jpa1999.0293

Elmore, R. W., Hoffmeister, G., Klein, R., & Marx, D. B. (2003). Corn greensnap from extreme wind is influenced by several factors. *Crop Management*, *2*(1), 1–12. https://doi.org/10.1094/CM-2003-1212-01-RS

Erndwein, L., Cook, D. D., Robertson, D. J., & Sparks, E. E. (2020). Field-based mechanical phenotyping of cereal crops to assess lodging resistance. *Applications in Plant Sciences*, *8*(8), e11382. https://doi.org/10.1002/aps3.11382

Fournier, C., & Andrieu, B. (2000). Dynamics of the elongation of internodes in maize (*Zea mays* L.): Analysis of phases of elongation and their relationships to phytomer development. *Annals of Botany*, *86*(3), 551–563. https://doi.org/10.1006/anbo.2000.1217

Hill, C. W. (2011). *Node and stalk breakage characteristics related to greensnap and maize genotypes*. Iowa State University.

Isnard, S., & Rowe, N. P. (2008). Mechanical role of the leaf sheath in rattans. *New Phytologist*, *177*(3), 643–652. https://doi.org/10.1111/j.1469-8137.2007.02308.x

Morrison, T. A., Kessler, J. R., & Buxton, D. R. (1994). Maize internode elongation patterns. *Crop Science*, *34*(4), 1055–1060. https://doi.org/10.2135/cropsci1994.0011183X003400040040x

Nelson, N., Stubbs, C. J., Larson, R., & Cook, D. D. (2019). Measurement accuracy and uncertainty in plant biomechanics. *Journal of Experimental Botany*, *70*(14), 3649–3658. https://doi.org/10.1093/jxb/erz279

Niklas, K. J. (1990). The mechanical significance of clasping leaf sheaths in grasses: Evidence from two cultivars of *Avena sativa*. *Annals of Botany*, *65*(5), 505–512. https://doi.org/10.1093/oxfordjournals.aob.a087962

Niklas, K. J. (1998). The mechanical roles of clasping leaf sheaths: Evidence from *Arundinaria tecta* (Poaceae) shoots subjected to bending and twisting forces. *Annals of Botany*, *81*(1), 23–34. https://doi.org/10.1006/anbo.1997.0513

Reneau, J. W., Khangura, R. S., Stager, A., Erndwein, L., Weldekidan, T., Cook, D. D., Dilkes, B. P., & Sparks, E. E. (2020). Maize brace roots provide stalk anchorage. *Plant Direct*, *4*(11), e00284. https://doi.org/10.1002/pld3.284

Robertson, D., Smith, S., Gardunia, B., & Cook, D. (2014). An improved method for accurate phenotyping of corn stalk strength. *Crop Science*, *54*(5), 2038. https://doi.org/10.2135/cropsci2013.11.0794

Robertson, D. J., Lee, S. Y., Julias, M., & Cook, D. D. (2016). Maize stalk lodging: Flexural stiffness predicts strength. *Crop Science*, *56*(4), 1711. https://doi.org/10.2135/cropsci2015.11.0665

Robertson, D. J., Smith, S. L., & Cook, D. D. (2015). On measuring the bending strength of septate grass stems. *American Journal of Botany*, *102*(1), 5–11. https://doi.org/10.3732/ajb.1400183

Sharman, B. C. (1942). Developmental anatomy of the shoot of *Zea mays* L. *Annals of Botany*, *6*(22), 245–282. https://doi.org/10.1093/oxfordjournals.aob.a088407

Stubbs, C., Baban, N., Robertson, D., Al-Zube, L., & Cook, D. (2018). Bending stress in plant stems: Models and assumptions. In A. Geitmann, & J. Gril (Eds.), *Plant biomechanics—From structure to function at multiple scales* (pp. 49–77). Springer. https://www.springer.com/gp/book/9783319790985

Stubbs, C., Larson, R., & Cook, D. D. (2020). Mapping spatially distributed material properties in finite element models of plant tissue using computed tomography. *Biosystems Engineering*, *200*, 391–399. https://doi.org/10.1016/j.biosystemseng.2020.10.008

Stubbs, C., Sun, W., & Cook, D. D. (2019). Measuring the transverse Young's modulus of maize rind and pith tissues. *Journal of Biomechanics*, *84*, 113–120. https://doi.org/10.1016/j.jbiomech.2018.12.028

Stubbs, C. J., Seegmiller, K., McMahan, C., Sekhon, R. S., & Robertson, D. J. (2020). Diverse maize hybrids are structurally inefficient at resisting wind induced bending forces that cause stalk lodging. *Plant Methods*, *16*, 1–15. https://doi.org/10.1186/s13007-020-00608-2

Tarara, J. M. (2000). Microclimate modification with plastic mulch. *HortScience*, *35*(2), 169–180. https://doi.org/10.21273/HORTSCI.35.2.169

Wu, W., Huang, J., Cui, K., Nie, L., Wang, Q., Yang, F., Shah, F., Yao, F., & Peng, S. (2012). Sheath blight reduces stem breaking resistance and increases lodging susceptibility of rice plants. *Field Crops Research*, *128*, 101–108. https://doi.org/10.1016/j.fcr.2012.01.002

Wu, W., & Ma, B. (2019). The mechanical roles of the clasping leaf sheath in cereals: Two case studies from oat and wheat plants. *Journal of Agronomy and Crop Science*, *206*, 118–129. https://doi.org/10.1111/jac.12362

How to cite this article: Hale, J., Webb, S., Hale, N., Stubbs, C., & Cook, D. (2023). Assessing axial and temporal effects of the leaf sheath on the flexural stiffness of large-grain stems. *Crop Science*, *63,* 822–832. https://doi.org/10.1002/csc2.20899